Table III. Comparison of Effective Quadrupole Moments Θ with Center-of-Mass Quadrupole Moments Θ′

Gas	Dipole moment, D	$10^{26}\Theta$, esu	g,[a] nuclear magneton	$10^{30}(\chi_{\parallel} - \chi_{\perp})$, emu	$10^{26}\Theta'$, esu	Z, Å	$10^{32}(A_{\parallel}' + 2A_{\perp}' + 10c\omega^{-1}G')$, esu
Carbonyl sulfide	0.712	-0.3 ± 0.1[b]	−0.02889[d]	−13.9[g]	−2.0	+1.2	−13
Nitrous oxide	0.167	-3.5 ± 0.3[c]	−0.086[e]	−18	−4.2	+2.1	−12
Carbon monoxide	0.112	-2.5 ± 0.3[c]	−0.2689[f]	−17	+0.4	−13	+14

[a] The sign of g for N_2O is not known; we have assumed it to be negative. [b] Using $\alpha_{\parallel} - \alpha_{\perp} = 5.34 \times 10^{-24}$ cm³, as measured for static fields: L. H. Scharpen, J. S. Muenter, and V. W. Laurie, *J. Chem. Phys.*, **46**, 2431 (1967). [c] Using values for $\alpha_{\parallel} - \alpha_{\perp}$ from ref 9. [d] J. W. Cederberg, C. H. Anderson, and N. F. Ramsey, *Phys. Rev.*, **136**, A960 (1964). [e] C. K. Jen, *ibid.*, **81**, 197 (1951). [f] I. Ozier, P. Yi, A. Khosla, and N. F. Ramsey, *J. Chem. Phys.*, **46**, 1530 (1967). [g] H. Taft and B. P. Dailey, *ibid.*, **48**, 597 (1968).

Negative charge in a plane at right angles to the molecular axis of a linear molecule contributes a positive amount to the quadrupole moment, while negative charge distributed along the molecular axis contributes negatively. Hence oxygen, with two more π electrons than nitrogen, has a less negative quadrupole moment. The positive sign of the quadrupole moment of ethylene may be attributed to the π character of the carbon–carbon double bond; acetylene is expected to have an even larger positive quadrupole moment.

Light Scattering by Crystalline Polystyrene and Polypropylene

A. E. M. Keijzers, J. J. van Aartsen, and W. Prins

Contribution from the Laboratory of Physical Chemistry, Technische Hogeschool, Delft, The Netherlands. *Received November 29, 1967*

Abstract: The light scattering by crystallizable polymers can yield valuable information regarding the crystallization behavior and the resulting crystalline morphology if (i) quantitative measurements are carried through and (ii) these are analyzed by using a physically realistic model. It is found that isotactic polystyrene and polypropylene samples can be adequately described as containing imperfect spherulites in which a number of perfectly spherulitic and a number of "random orientation" crystallites are present. Growth rates, sizes, and the number of spherulites follow easily from the scattering data. The internal structure of the imperfect spherulites can be characterized by the birefringence of the perfectly spherulitic crystallites plus a density correlation distance, two orientation correlation distances, and the mean polarizability and anisotropy fluctuations of the "random orientation" crystallites. It is found that in isotactic polystyrene the crystallinity of the spherulites is a decreasing function of the radius. In the case of isotactic polypropylene it could be shown that the secondary crystallization is not spherulitical, in contradistinction to the primary crystallization.

In 1949 Debye and Bueche[1] demonstrated how measurements of the light scattering by an amorphous polymer could be used to obtain a density correlation function $\gamma(r)$ describing the supermolecular order in the samples. Since that time several investigators,[2] notably Stein,[3] have extended this method of investigation to other, more complicated, polymer systems. In the present article we will demonstrate the usefulness of *quantitative* light-scattering data for studying the crystallization behavior and the resulting supermolecular order in crystalline polymers. Our samples consisted of bulk crystallized isotactic polystyrene and polypropylene which upon microscopic examination are found to contain spherulitic aggregates of crystallites.

Necessary conditions for such a quantitative study are (i) a light-scattering photometer of high resolution, capable of measuring down to very small angles, and (ii) a physically realistic model for the structure of the spherulites. The first requirement offers no serious difficulties; a convenient instrument, constructed in our laboratory, has been described previously.[4] It consists essentially of a finely collimated primary beam and a photomultiplier–detector, mounted on a swivelling arm. With this combination one can measure down to 30′ from the primary beam. The second requirement implies that maximum information can only be obtained if some previous knowledge of the morphology is available through other experimental techniques. This requirement derives from the fact that there is little use introducing a set of correlation functions which formally describe the structure. In the first place the physical interpretation of such a set of functions remains dubious, and, secondly, the experimental results do not always allow reliable Fourier inversions which are needed to yield the functions.

In the recent past, two main models have been described in the literature. In one[5,6] the spherulite is considered to be perfect; *i.e.*, all crystallites are con-

(1) P. Debye and A. M. Bueche, *J. Appl. Phys.*, 20, 518 (1949).
(2) M. Goldstein and E. R. Michalik, *ibid.*, **26**, 1450 (1955).
(3) R. S. Stein and P. R. Wilson, *ibid.*, **33**, 1914 (1962).
(4) A. E. M. Keijzers, J. J. van Aartsen, and W. Prins, *ibid.*, **36**, 2874 (1965).
(5) R. S. Stein and M. B. Rhodes, *ibid.*, **31**, 1873 (1960).
(6) J. J. van Aartsen, "The Scattering of Light by Deformed Three-Dimensional Spherulites," O.N.R. Report No. 83, Polymer Research Institute, University of Massachusetts, Amherst, Mass., March 1, 1966.

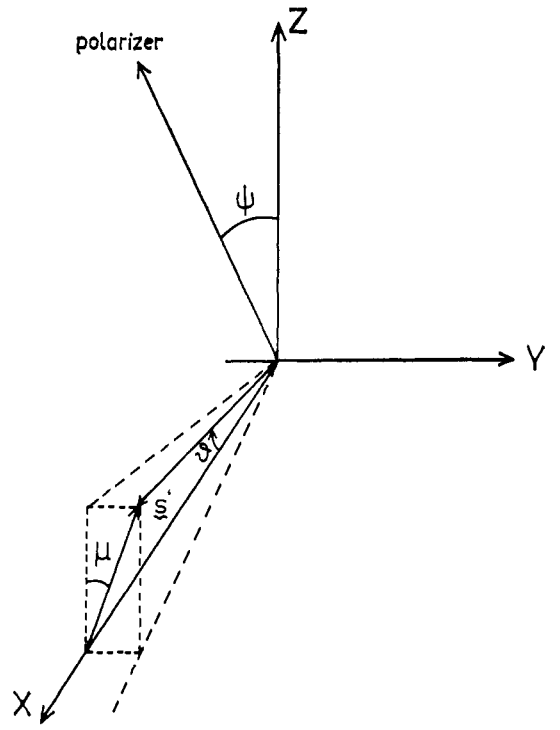

Figure 1. Diagram defining the directions of the polarizer axis and the scattered beam (s'). The primary beam runs along the X axis.

sidered to have a fixed orientation of the optical axis with respect to the radius of the spherulite. In the other,[3] a "random orientation" correlation is introduced. Its essential content is that the orientation correlation is assumed to be a distance function only. Obviously, this latter model should not be applicable in a crystalline sample in which the spherulites are well developed. Light and electron microscopy[7-10] studies have shown that in a real spherulite fibrillar crystals grow out from the center in radial direction, which on their way to the perimeter branch out. The center of the spherulite contains sheaflike assemblies of crystallites, which are spherulitically irregular. The role of secondary crystallization in between the fibrils has been recognized, but the resulting precise crystallite arrangement is unknown.

On the basis of these considerations, we introduce a "combination" model for the calculation of the light scattering, in which the two main features of the actual morphology are present. The spherulite is thus considered to contain a certain number of perfectly spherulitic crystallites and a certain number of "random orientation" crystallites.

The analysis shows that it is possible in this case to arrange the quantitative experimental data in such a way that the two contributions to the scattering can be separated. The light-scattering experiments on our samples then allow several conclusions as regards their crystallinity and the nature of the secondary crystallization.

(7) H. D. Keith and F. J. Padden, *J. Appl. Phys.*, 34, 2409 (1963).
(8) P. H. Geil, "Polymer Single Crystals," John Wiley and Sons, Inc., New York, N. Y., 1963.
(9) H. D. Keith and F. J. Padden, *J. Polymer Sci.*, 39, 101 (1959).
(10) H. E. Buchley, "Crystal Growth," John Wiley and Sons, Inc., New York, N. Y., 1951.

The scattering is calculated by simply adding the intensities of the light scattering by the perfectly spherulitical crystallites and the nonspherulitic ("random orientation") crystallites; mutual interference effects are not considered.

Pure spherulitic as well as "random orientation" scattering have already been calculated by Stein and coworkers.[3,5,6] In carrying out his calculations, Stein used a vector **o** (indicating which polarization direction is transmitted by a Polaroid analyzer filter, perpendicular to the primary beam), which is only valid for small angles. The calculations have therefore been repeated with the aid of a correctly defined vector **o** (see Appendix I), valid for larger angles too.

For the spherulitic part, the scattered intensities, expressed in terms of Rayleigh ratios, are shown in eq 1 and 2 for the parallel and crossed position of analyzer

$$R_{||}^{sf} = \frac{\kappa}{R_p^2 \cos^2(\mu+\psi) + R_q^2 \cos^2\theta_p^* \sin^2(\mu+\psi)} \times [A\cos^2(\theta/2)\cos^2(\mu+\psi) + B\{\cos\theta\cos^2(\mu+\psi) + \cos\theta_q^* \sin^2(\mu+\psi)\}]^2 \quad (1)$$

$$R_{+}^{sf} = \frac{\kappa \sin^2(\mu+\psi)\cos^2(\mu+\psi)}{R_p^2 \sin^2(\mu+\psi) + R_q^2 \cos^2\theta_p^* \cos^2(\mu+\psi)} \times [A\cos^2(\theta/2) + B(\cos\theta - \cos\theta_p^*)]^2 \quad (2)$$

and polarizer, respectively. The angles θ (scattering angle), μ, and ψ are defined in Figure 1, while R_p, R_q, and θ_p^* will be explained in Appendix I. The other quantities are

$$\kappa = N_{sf}\left[\frac{4}{3}\pi R_{sf}^3\right]^2 \frac{\pi^2}{\lambda_0^4} \quad (3)$$

$$A = 12\pi(\alpha_r - \alpha_t)\left[\frac{4\sin U - U\cos U - 3\,\mathrm{Si}\,U}{U^3}\right] \quad (4)$$

$$B = 12\pi\left[\alpha_t\left\{\frac{\sin U - U\cos U}{U^3}\right\} + (\alpha_r - \alpha_t) \times \left\{\frac{\mathrm{Si}\,U - \sin U}{U^3}\right\}\right] \quad (5)$$

$$U = \frac{4\pi \sin(\theta/2)}{\lambda} R_{sf} \quad (6)$$

where N_{sf} is the number of spherulites per cm^3; R_{sf} is the radius of the spherulites; λ and λ_0 are the wavelengths of the light in the medium and *in vacuo*, respectively; α_r and α_t are the polarizabilities of the spherulite in radial and tangential direction, respectively; and Si is the symbol for $\int_0^U (\sin x/x)dx$.

The scattered intensities from the "random orientation" part for the parallel and crossed position of polarizer and analyzer, respectively, are given by

$$R_{||}^{rand} = [R_p^2\cos^2(\mu+\psi) + R_q^2\cos^2\theta_p^*\sin^2(\mu+\psi)]^{-1} \times [Q\{\cos^2(\mu+\psi) + \cos^2\theta_p^*\sin^2(\mu+\psi)\} + (O-Q) \times \{\cos\theta\cos^2(\mu+\psi) + \cos\theta_p^*\sin^2(\mu+\psi)\}^2] \quad (7)$$

$$R_{+}^{rand} = [R_p^2\sin^2(\mu+\psi) + R_q^2\cos^2\theta_p^* \times \cos^2(\mu+\psi)]^{-1}[Q\{\sin^2(\mu+\psi) + \cos^2\theta_p^* \times \cos^2(\mu+\psi)\} + (O-Q)(\cos\theta - \cos\theta_p^*)^2 \times \sin^2(\mu+\psi)\cos^2(\mu+\psi)] \quad (8)$$

where

$$O = K\left[\langle\eta^2\rangle\int_0^\infty \gamma(r)\frac{\sin hr}{hr}r^2\,dr + \frac{4}{45}\delta^2 \times \int_0^\infty f(r)\mu(r)\frac{\sin hr}{hr}r^2\,dr\right] \quad (9)$$

$$Q = \frac{1}{15}K\delta^2\int_0^\infty f(r)\mu(r)\frac{\sin hr}{hr}r^2\,dr \quad (10)$$

$$K = \frac{64\pi^5}{\lambda_0^4} \quad (11)$$

$$\mu(r) = 1 + \frac{\langle\eta^2\rangle}{\alpha^2}\gamma(r) \quad (12)$$

$\langle\eta^2\rangle$ is the mean-square polarizability fluctuation, δ the mean anisotropy, and α the mean polarizability of the sample; $\gamma(r)$ and $f(r)$ are the density correlation and orientation correlation functions, respectively, and $h = 4\pi\sin(\theta/2)/\lambda$.

As mentioned before, the total scattering by the sample is obtained by adding the intensities from the spherulitic and the "random orientation" part. The quantities O, Q, and κA^2 are obtained from the four different measured scattering components: $(V_v)_{tot}$, $(H_h)_{tot}$, $(H_v)_{tot}$, and $(K_d)_{tot}$ (K_d denotes the component, measured with crossed polarizer and analyzer at $\mu = 90°$ and $\psi = 45°$. V_v, H_h, and H_v have the usual meaning); a detailed description of the separation of the measured components into O, Q, and κA^2 is given in Appendix II.

Experimental Section

Light-Scattering Apparatus. All light-scattering measurements have been carried out with the light-scattering photometer, already described by the authors;[4] measurements can only be made in the horizontal plane, *i.e.*, in the $\mu = 90°$ position. With the aid of an auxiliary apparatus (see Figure 2), it was possible to measure any desired scattering component. In this apparatus two Polaroid filters, coupled by means of wormgear, can be rotated through an angle ψ simultaneously. If, for example, the polarizer and analyzer are crossed (see Figure 2), they are kept crossed for any value of ψ (for the K_d component, ψ should be 45° with crossed polarizer and analyzer). The measurements have been corrected for turbidity of the sample, internal scattering angle, etc., in the way described by Stein and Keane.[11] Corrections for the reflection of the scattered ray have not been made, because these have already been accounted for in the vector **o**, used in the theoretical calculations (see Appendix I).

Sample Preparation. Isotactic polystyrene and isotactic polypropylene were kindly supplied by the Central Research Institute of the AKU, Arnhem, The Netherlands, and by Shell Plastics Laboratory, Delft, The Netherlands. According to the statements of the suppliers, the viscosity and number-average molecular weights of polystyrene were 330,000 and 185,000, respectively; the viscosity-average molecular weight of polypropylene (sample N 577) was 400,000.

For the preparation of the samples, the molten polymer was first pressed between two quartz slides of 3-mm thickness. The slides were separated by two copper strips of required thickness, ensuring a plane-parallel polymer film. The melt was kept at the required temperature (polystyrene 265°, polypropylene 210°) for 1 hr so as to reduce macroscopic orientation, resulting from the streaming patterns, caused by pressing together the quartz slides. After a sometimes required quench, the sample was put quickly into the crystallization oven. The crystallization oven consisted of two copper blocks, through which by way of a series of channels a thermally regulated liquid (silicone oil) was circulated from a thermostat. Between these two blocks a copper plate was inserted out of which the oven cavity had been sawed. The cavity had somewhat larger dimensions than the quartz slides with the polymer. The temperature in the oven cavity could be kept constant to at least 0.1°. After the crystallization the sample was quenched rapidly in a liquid of the required temperature (melting acetone for −95° and water for temperatures from 0 to 100°).

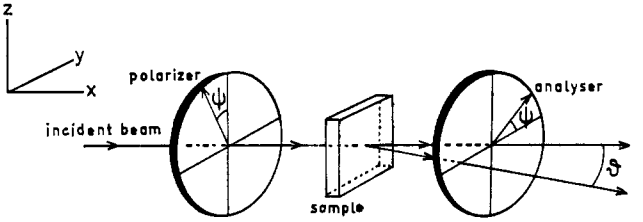

Figure 2. Schematic diagram of the coupled polarizer and analyzer.

Analysis of the Scattering Data. The quantity κA^2 has a maximum at $U = 4.10$. So with the aid of eq 6 the mean radius of the spherulites, R_{sf}, can be calculated from the value of sin $(\theta/2)$ at which κA^2 is maximal.

The value of κA^2 in the maximum yields the absolute value of the polarizability difference $\alpha_r - \alpha_t$, if the number of spherulites per cm³, N_{sf}, is known (see eq 3 and 4 and next section). The birefringence of the spherulites $(\Delta n)_{sf}$ (the difference of the refractive indices in radial and tangential direction) can be found from the differentiated Lorenz–Lorentz equation

$$(\Delta n)_{sf} = \frac{2\pi(n^2+2)^2}{9n}(\alpha_r - \alpha_t) \quad (13)$$

where n is the mean refractive index.

If a plot of $\ln(O - {}^4/_3Q)$ *vs.* $\sin^2(\theta/2)$ is linear (which is the case for all measured samples), Keijzers, van Aartsen, and Prins[4] have shown that the density correlation function $\gamma(r)$ is Gaussian

$$\gamma(r) = \exp(-r^2/a^2) \quad (14)$$

where a is a characteristic correlation distance. From eq 9 and 10 it follows that for such a Gaussian function

$$(O - {}^4/_3Q) = {}^1/_4K\langle\eta^2\rangle a^3\sqrt{\pi}\exp(-h^2a^2/4) \quad (15)$$

Thus, a and $\langle\eta^2\rangle$ can be calculated from the slope and the intercept in the plot of $\ln(O - {}^4/_3Q)$ *vs.* h^2 (or $\sin^2(\theta/2)$).

The orientation correlation function $f(r)$ can be determined in a way similar to the determination of $\gamma(r)$. For polypropylene it has already been found earlier[4] that $f(r)$ can be thought to consist of two different Gaussian functions

$$f(r) = x\exp(-r^2/b^2) + (1-x)\exp(-r^2/c^2) \quad (16)$$

in which b and c are characteristic correlation distances. For the solution of eq 10 one needs to know $\mu(r)$ too. Because for all samples considered in this investigation, $\langle\eta^2\rangle/\alpha^2 < 10^{-4}$ and $\gamma(r) \leq 1$, one has to a good approximation $\mu(r) = 1$ for all values of r (see eq 12). Using eq 16 and putting $\mu(r) = 1$, one finds from eq 10

$$Q = \frac{1}{15}K\delta^2\left[\frac{xb^3\sqrt{\pi}}{4}\exp\left(-\frac{h^2b^2}{4}\right) + \frac{(1-x)c^3\sqrt{\pi}}{4}\exp\left(-\frac{h^2c^2}{4}\right)\right] \quad (17)$$

Thus, if there is a relatively large difference between b and c, the course of a plot of $\ln Q$ *vs.* h^2 (or $\sin^2(\theta/2)$) will be linear at small and at large values of h^2. From the slopes of both linear parts of the curve, the correlation distances c and b can be determined; the intercepts, obtained by extrapolation of both linear parts to $h^2 = 0$, can be used to calculate x and δ.

Results

Table I shows the thermal history of the polystyrene samples. Following Boon[12] the samples were first

(11) R. S. Stein and J. J. Keane, *J. Polymer Sci.*, 17, 21 (1955).

(12) J. Boon, "Kristallisatiekinetiek van Isotactisch Polystyreen," Thesis, Delft, The Netherlands, 1966; see also J. Boon, *J. Polymer Sci.*, C16, 1739 (1967).

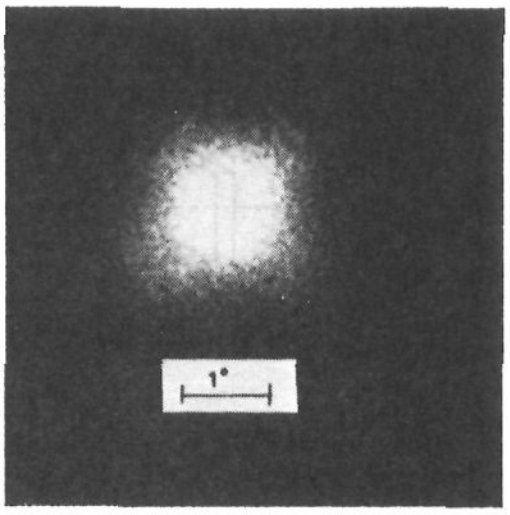

Figure 3. Scattering pattern (for the crossed position of polarizer and analyzer) of quenched (to 0°) polypropylene (sample pp2).

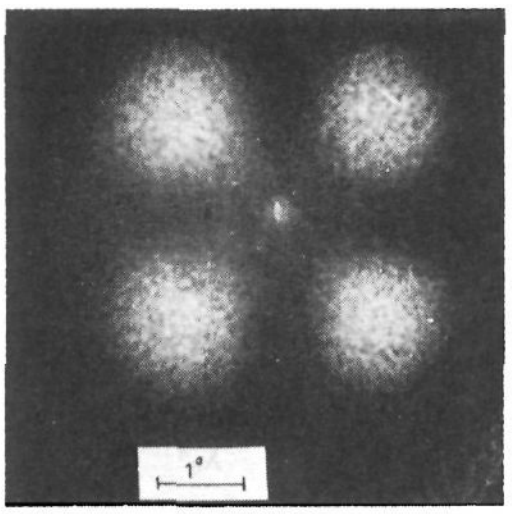

Figure 4. Scattering pattern (for the crossed position of polarizer and analyzer) of deeply quenched (to −95°) polypropylene (sample pp3).

brought from the melt at T_1 to a lower temperature T_2 in order to create subcritical nuclei. Crystallization was subsequently carried out at T_x. Samples ps1, ps2, ps3, and ps5 were quenched to room temperature after a time t_x chosen in such a way that the sample was not yet filled with spherulites; sample ps4, on the other hand, was crystallized until the whole volume was filled with spherulites of the same size as in sample ps5.

Table I. Thermal History of the Polystyrene Samples

Code	T_1, °C	t_1, min	T_2, °C	t_2, min	T_x, °C	t_x, min	N_{sf}, cm^{-3}
ps1	265	60	20	10	140	15	1.1×10^{11}
ps2	265	60	20	10	140	20	1.1×10^{11}
ps3	265	60	20	10	140	25	1.1×10^{11}
ps4	265	60	98	30	140	240	0.7×10^{9}
ps5	265	60	...	...	140	140	1.7×10^{7}

As we will show below, our light-scattering measurements yield the radii of the spherulites in a straightforward manner, even if the microscopic determination fails. By studying the radii as a function of t_x, the radial growth rate, v_r, could be quite accurately determined. At 140°, $v_r = 0.044$ μ/min. An estimate of the number of spherulites, N_{sf}, was obtained by putting $N_{sf}(4\pi R_{sf}^3/3)$ equal to unity in the completely crystallized samples. These numbers, which are listed in Table I, check quite well with the number of nuclei as determined dilatometrically by Boon.[12] This confirms the picture of the crystallization of isotactic polystyrene in which an intermediate quench can be used to regulate the number of spherulites in the sample.

Table II shows the thermal history of the polypropylene samples. Here the samples were brought directly from the melt (T_1) to a temperature T_4. Crystallization is so fast in this system that it proved impossible to follow the polystyrene procedure. According to Padden and Keith[13] and von Falkai and Stuart,[14,15] the radial growth rate at 110° is 130 μ/min and the number of nuclei about 10^8–10^9 cm^{-3}, so that in about 2 sec the whole sample is crystallized. At lower temperatures the number of nuclei will still increase and the growth rate probably too. Samples containing "free" spherulites could thus not be obtained.

(13) F. J. Padden and H. D. Keith, *J. Appl. Phys.*, **30**, 1479 (1959).
(14) B. von Falkai and H. A. Stuart, *Kolloid-Z.*, **162**, 138 (1959).
(15) B. von Falkai, *Makromol. Chem.*, **41**, 86 (1960).

Figures 3 and 4 show the photographic scattering patterns of two polypropylene samples between crossed polaroids obtained by quenching to two different T_4 temperatures. It is of interest to observe that in Figure 3 the typical four-leaf-clover pattern of a spherulite is almost swamped by a larger amount of random orientation scattering. The same, but then in a quantitative manner, is shown in Figures 5 and 6. In these figures the separation into spherulitic scattering ($I = \kappa A^2$) and random orientation scattering ($I = Q$) is achieved in the way indicated in the previous section.

Table II. Thermal History of Polypropylene Samples

Code	T_1, °C	t_1 min	T_4, °C	t_4, min	N_{sf}, cm^{-3}
pp1	210	60	98	30	0.89×10^{8}
pp2	210	60	0	30	1.06×10^{8}
pp3	210	60	−95	30	4.61×10^{8}

A test on the validity of the "combination" model is shown in Table III. The scattering R_+^{tot} of an arbitrary sample (pp3) was measured at $\theta_u = 5°$ between crossed polaroids, as a function of the angle ψ. After subtraction of the spherulitic scattering, R_+^{sf}, calculated according to the ψ dependence given by eq 2, it is found that the random orientation scattering, R_+^{rand}, is independent of ψ, as should indeed be the case at small θ_u.

Table III

ψ	R_+^{tot}	R_+^{sf}	R_+^{rand}
0	36.0	0	36.0
10	47.8	12.3	35.5
20	80.5	43.8	36.7
30	115.2	79.6	35.6
40	139.3	102.9	36.4
45	142.1	106.1	36.9
50	139.1	102.9	36.2
60	115.6	79.6	36.0
70	80.2	43.8	36.4
80	47.9	12.3	35.6
90	36.0	0	36.0

Figures similar to Figures 5 and 6 have been obtained for all samples. The density correlation function $\gamma(r)$ $(=\exp(-r^2/a^2))$ is obtained from plots of ln

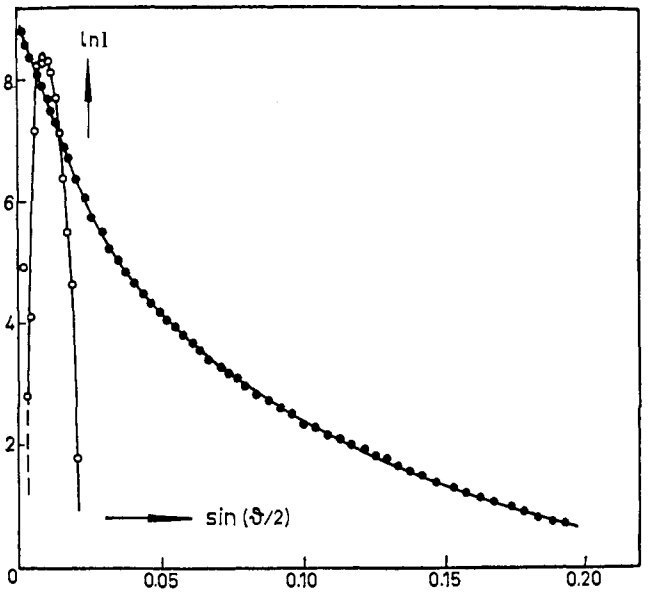

Figure 5. Scattering curves of sample pp2: ● = ln Q, ○ = ln κA^2.

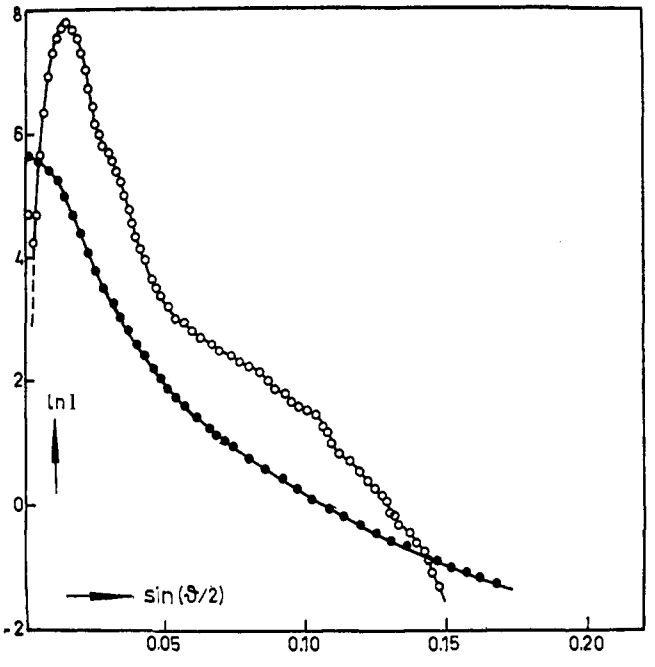

Figure 6. Scattering curves of sample pp3: ● = ln Q, ○ = ln κA^2.

($O - {}^4/_3 Q$) *vs.* $\sin^2(\theta/2)$. Figure 7 shows an example for several polystyrene samples. The orientation correlation function, $f(r) = x \exp(-r^2/b^2) + (1 - x) \exp(-r^2/c^2)$, is obtained from ln Q. The straight lines in Figure 7 demonstrate that in samples ps1, ps2, and ps3 $f(r) = \exp(-r^2/b^2)$ ($x \simeq 1$); sample ps4 (as well as ps5) does not yield a single straight line over the whole angular range so that there $x \neq 1$. A more pronounced example of this latter behavior is shown in Figure 8 for samples pp1 and pp3.

All characteristic parameters which follow from this quantitative light-scattering analysis are listed in Table IV. A comparison of R_{sf} and the correlation distance a shows that these quantities are related: a larger R_{sf} also means a larger a. This is indeed to be expected.

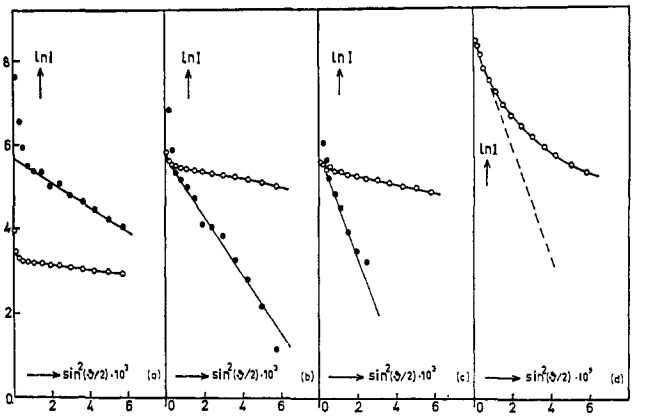

Figure 7. Random orientation part of the scattering: a = ps1, b = ps2, c = ps3, d = ps4; ● = ln ($O - 4/3\ Q$), ○ = ln Q.

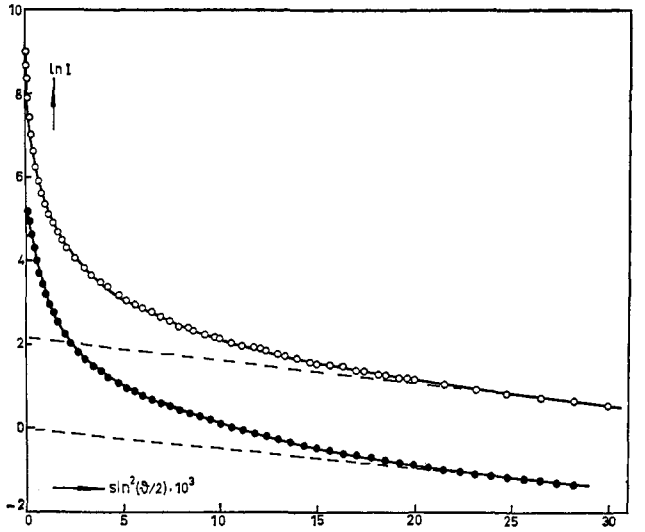

Figure 8. The anisotropic part (ln Q) of the "random orientation" scattering: ○ = pp1, ● = pp3.

The value of b seems to be a constant for each polymer (ps, $b = 0.44\ \mu$; pp, $b = 0.39\ \mu$). It is very plausible to consider b as a measure of the spherulitically irregular center of the spherulite. The correlation distance c should then originate from the irregularity of the whole spherulite. For the very small spherulites of ps1, ps2, and ps3, no c value is detectable because in these cases c is of the same order of magnitude as b (or because the contribution from the $(1 - x)$ term is so small that it vanishes). Samples ps4 and ps5 show that the c scattering cannot be due to impingement of spherulites. In

Table IV

Sample	R_{sf}, μ	a, μ	b, μ	c, μ	x	$\langle \eta^{2\,1/2} \rangle \times 10^4$	$\delta \times (\alpha_r - \alpha_t)$ 10^3	$\times 10^3$
ps1	0.65	0.92	0.42	...	1	6.25	2.33	5.92
ps2	0.88	1.44	0.51	...	1	3.25	5.39	6.49
ps3	1.02	1.94	0.54	...	1	2.18	4.74	4.30
ps4	6.27	...	0.42	1.95	0.73	...	6.12	1.80
ps5	6.30	...	0.41	2.23	0.72	...	0.25	...
pp1	13.9	4.80	0.42	6.57	0.73	3.64	1.59	0.218
pp2	13.1	4.07	0.37	4.92	0.83	3.24	1.92	0.200
pp3	8.03	3.35	0.38	3.17	0.66	0.32	0.63	0.304

both samples a similar c value is found, although in ps5 the spherulites do not touch each other.

It is of interest to point out that in a previous analysis of the light scattering of polypropylene the spherulitic part of the scattering was completely neglected.[4] The sample was similar to pp2. The pattern shown in Figure 3 and the quantitative data in Figure 5 show that indeed in this case the random orientation scattering swamps the spherulitic scattering. Neglect of the spherulitic scattering in this case then is not serious. In most cases, however, the spherulitic scattering is of paramount importance. Figure 6 even shows some shoulders in the spherulitic scattering curve, which indicate the remains of higher order diffraction maxima. This shows that the size distribution of the spherulites before impingement must have been quite narrow.[16]

Turning now to the polarizability ($\langle\eta^2\rangle^{1/2}$) and anisotropy ($\delta$) fluctuations, as listed in Table IV, we observe the following: $\langle\eta^2\rangle^{1/2}$ decreases in the sequence ps1, ps2, ps3. Since in our model $\langle\eta^2\rangle^{1/2}$ should reflect the difference in mean refractive index of spherulite and surrounding medium, this quantity should diminish the larger the portion of the volume which is filled by spherulites. Considering next the mean anisotropy δ, it should be remembered that the polystyrene samples differ in the volume which the spherulites occupy. The fraction of crystalline material, f, can be calculated from the observed growth rate v_r and N_{sf} through the relation[17]

$$-\ln(1-f) = 4\pi N_{sf} V_0 v_r t/3V_s \qquad (18)$$

where V_0 and V_s are the specific volumes of the amorphous and spherulitical phase, respectively.[18] Equation 18 is valid if the number of nuclei is constant, which is true in our case.

Excluding ps5, we then find upon comparing δ/f for our polystyrene samples a decrease of δ/f with increasing radius of the spherulites (Table V). This can

Table V

Sample	ps1	ps2	ps3	ps4	ps5
$(\delta/f) \times 10^3$	19.4	22.0	9.3	6.2	14.0
R_{sf}, μ	0.65	0.88	1.02	6.27	6.30

be taken as an indication that the crystallinity of the nonspherulitical part within the spherulites decreases with increasing radius. A similar conclusion can be drawn from the decrease of $\alpha_r - \alpha_t$, which refers to the spherulitically arranged crystallites. Our $\alpha_r - \alpha_t$ values when converted to $(\Delta n)_{sf}$ (see eq 13) are in good agreement with microscopic determinations of this quantity by Picot, Weill, and Benoit.[19]

Such a radial dependence of the crystallinity is understandable because the growing spherulite becomes more open toward the perimeter (in spite of some branching), resulting in a decrease of crystallinity per volume unit. This finding invalidates the usual procedure in dilatometric crystallization studies where one assumes a constant crystallinity within the spherulite.

Hoshino, *et al.*,[20] have studied the crystallization of polypropylene dilatometrically, microscopically, and by means of X-ray diffraction. They concluded, in accordance with other studies on polymer crystallization, that there must be a primary spherulitic crystallization followed by a secondary crystallization, which might or might not be spherulitic. Their data are compatible with a theory which yields a decreasing crystallinity with increasing radius of the spherulite as a result of two consecutive crystallization processes. Our data on polystyrene and polypropylene indicate the same radial decrease in crystallinity.

In the polypropylene series, we find $\langle\eta^2\rangle^{1/2}$ to be much smaller in sample pp3 than in the other two. This means that in pp3 we have a lower refractive index of the scattering units with respect to the surrounding. It seems logical to connect this with a smaller total crystallinity of the spherulites in the case of pp3. The smaller value of δ and the roughly unchanged $\alpha_r - \alpha_t$ value would then indicate that the lower crystallinity resides mainly in the nonspherulitically crystallized material within the spherulite. The $\alpha_r - \alpha_t$ values, when converted to $(\Delta n)_{sf}$, are in good correspondence with the birefringence of type I and II spherulites as determined by Padden and Keith.[13] All our samples showed spherulites of the mixed type under the microscope.

The considerably smaller crystallinity of the random orientation part of pp3 can be explained by assuming that the secondary, nonspherulitic, crystallization was suppressed in sample pp3 because of the exceptionally deep quench to $-95°$. Since $(\Delta n)_{sf}$ hardly changes, secondary crystallization must lead to new crystallites rather than to a gradual perfectioning of the existing primary spherulitic crystallites. In fact, the widths of the X-ray diffraction maxima of samples pp2 and pp3 show that the secondary crystallites present in pp3 are much more perfect or larger than the primary spherulitic crystallites.

Since our measurements were performed on unfractionated polypropylene, it is conceivable that the secondary process occurring between the fast grown spherulitic fibrils represents the crystallization of the lower molecular weight tail of the distribution.

Conclusions

From the preceding it follows that a quantitative light-scattering analysis on the basis of a physically realistic model for the morphology of crystalline polymer samples is capable of providing the following useful information.

(1) The light scattering of isotactic polystyrene and polypropylene can be described very well by a model consisting of imperfect spherulites, containing randomly correlated crystallites in addition to perfectly spherulitically arranged crystallites.

(2) With the aid of this model it is possible to determine accurately the growth rates and the sizes of the spherulites from the scattering, often even in those cases

(16) A. E. M. Keijzers, "Light Scattering by Crystalline Polystyrene and Polypropylene," Thesis, Delft, The Netherlands, 1967.

(17) M. Avrami, *J. Chem. Phys.*, 7, 1303 (1939); 8, 212 (1940); 9, 177 (1941).

(18) Although one should really use the volume fraction of spherulites, ϕ_s, instead of the mass fraction, f, we have chosen to take the unknown $V_s = V_c$ in which case $\phi_s = f$. The error introduced in this way is of the order of a few per cent only, in view of the fact that V_c/V_s must be lower than 1.05, calculated for a completely crystalline spherulitic part.

(19) C. Picot, G. Weill, and H. Benoit, unpublished manuscript, C.R.M., Strasbourg.

(20) S. Hoshino, E. Meinecke, J. Powers, and R. S. Stein, *J. Polymer Sci.*, A3, 3041 (1965).

where it is impossible to do so by the current optical methods.

(3) In accordance with dilatometric results, the number of nuclei during the crystallization of polypropylene seems to be constant.

(4) For polystyrene, the crystallinity of the spherulites appears to decrease with increasing radius.

(5) The mean value of the birefringence of spherulites can be determined by means of light scattering.

(6) The secondary crystallization in the case of polypropylene is not spherulitic. It must be ascribed to the formation of new crystallites and not to the perfection of already existing crystallites.

Appendix I

The Vector o.[21] In light-scattering theory one always needs to specify a vector **o**, indicating which polarization direction is transmitted by the analyzer. According to Baxter,[22] for a Polaroid (Type HN 22) analyzer filter in the general case of oblique incidence, the transmitted direction should be perpendicular to the propagation direction of the ray (*i.e.*, in light-scattering theory, the direction of the scattered ray) and has to be parallel to the plane through the transmittance axis of the Polaroid filter, perpendicular to the filter material (analyzer). Because of reflections of the scattered ray at several interfaces, changes in this polarization direction and in the intensity occur. Taking this into account and using the reflection formulas of Fresnel, one can find the vector **o** (not a unit vector) to be

$$\mathbf{o} = \frac{1}{N}[x_1\mathbf{i} + x_2\mathbf{j} + x_3\mathbf{k}] \tag{19}$$

where **i**, **j**, and **k** are unit vectors in the X, Y, and Z direction, respectively (see Figures 1 and 2). The quantities N, x_1, x_2, and x_3 are given by

$$N = [R_p^2 \cos^2 \xi + R_q^2 \cos^2 \theta_p^* \sin^2 \xi]^{1/2} \tag{20}$$

$$x_1 = -\cos \xi \sin \theta \tag{21}$$

$$x_2 = \cos \xi \cos \theta \sin \mu - \cos \theta_p^* \sin \xi \cos \mu \tag{22}$$

$$x_3 = \cos \xi \cos \theta \cos \mu - \cos \theta_p^* \sin \xi \sin \mu \tag{23}$$

where $\xi = \mu + \psi$ for the parallel position of polarizer and analyzer and $\xi = 90° - (\mu + \psi)$ for the crossed position of polarizer and analyzer; ψ is the angle between the transmittance axis of the polarizer and the Z axis; μ and θ together determine the direction of the scattered ray as shown in Figure 1.

$$R_p^2 = (1 - r_{sp}^2)(1 - r_{kp}^2)^2 \tag{24}$$

$$R_q^2 = (1 - r_{sq}^2)(1 - r_{kq}^2)^2 \tag{25}$$

(21) A detailed calculation of the vector **o** has been given by Keijzers.[16]

(22) L. Baxter, *J. Opt. Soc. Am.*, **46**, 435 (1956).

$$\cos \theta_p^* = \cos \theta_p \cos (\theta_p - \theta_u) \tag{26}$$

$$r_{sp} = \frac{\tan(\theta - \theta_u)}{\tan(\theta + \theta_u)} \tag{27}$$

$$r_{kp} = \frac{\tan(\theta_p - \theta_u)}{\tan(\theta_p + \theta_u)} \tag{28}$$

$$r_{sq} = \frac{\sin(\theta - \theta_u)}{\sin(\theta + \theta_u)} \tag{29}$$

$$r_{kq} = \frac{\sin(\theta_p - \theta_u)}{\sin(\theta_p + \theta_u)} \tag{30}$$

where θ, θ_u, and θ_p are the scattering angles in the sample, in air, and in the Polaroid filter, respectively.

Appendix II

As any component of the total scattering by the sample can be formed by adding the corresponding scattering components of the spherulitic and the "random orientation" part, the following equations can be found with the aid of eq 1, 2, 7, and 8.

$$i_1 = R_q^2(V_v)_{tot} = O + \kappa B^2 \tag{31}$$

$$i_2 = R_p^2(H_h)_{tot} = Q + (O - Q + \kappa B^2)\cos^2\theta + \kappa A^2 \cos^4(\theta/2) + 2\kappa AB \cos^2(\theta/2)\cos\theta \tag{32}$$

$$i_3 = 2(R_p^2 + R_q^2 \cos^2\theta_p^*)(K_d)_{tot} = 2Q(1 + \cos^2\theta_p^*) + (O - Q + \kappa B^2)(\cos\theta - \cos\theta_p^*)^2 + \kappa A^2 \cos^4(\theta/2) + 2\kappa AB \cos^2(\theta/2)(\cos\theta - \cos\theta_p^*) \tag{33}$$

$$i_4 = R_p^2(H_v)_{tot} = Q \tag{34}$$

With the aid of the following two quantities T and V

$$T = (i_2 - i_4) - \cos^2\theta(i_1 - i_4) = \kappa A^2 \cos^4(\theta/2) + 2\kappa AB \cos^2(\theta/2)\cos\theta \tag{35}$$

$$V = \cos^2\theta[i_3 - 2(1 + \cos^2\theta_p^*)i_4] - (\cos\theta - \cos\theta_p^*)^2 \times (i_2 - i_4) = \kappa A^2 \cos^4(\theta/2)[\cos^2\theta - (\cos\theta - \cos\theta_p^*)^2] + 2\kappa AB \cos^2(\theta/2)[(\cos\theta - \cos\theta_p^*) \times \cos^2\theta - \cos\theta(\cos\theta - \cos\theta_p^*)^2] \tag{36}$$

κA^2 and κAB can be found from

$$\kappa A^2 = \frac{V - T\cos\theta_p^*(\cos\theta - \cos\theta_p^*)}{\cos^4(\theta/2)\cos\theta_p^*\cos\theta} \tag{37}$$

$$\kappa AB = \frac{T\cos\theta_p^*(2\cos\theta - \cos\theta_p^*) - V}{2\cos^2(\theta/2)\cos\theta_p^*\cos\theta} \tag{38}$$

So in this way κA^2 and κAB follow from experimental quantities; κB^2 can subsequently be calculated and used to determine O from eq 31, while Q is directly given by eq 34.